Calibration of an Integrated 1500nm Tunable Semiconductor Laser for OCT

Rastko Pajković, Kevin Williams and Erwin Bente

Photonic Integration Group, Department of Electrical Engineering, Eindhoven University of Technology, PO Box 513, 5600 MB Eindhoven, The Netherlands.

We investigate a widely tunable integrated semiconductor laser for application in optical coherence tomography. Calibration results are presented and the causes for long term calibration drift are discussed. We discuss the influence of electrical cross-talk in this recent ring laser on tuning precision and stability.

Introduction

Integrating an optical coherence tomography (OCT) system on a chip using photonic integration technology [1] opens the door for biomedical and industrial applications that require compact and robust imaging systems [2]. A study of the stepwise tuning of a widely tunable integrated semiconductor laser to be used for OCT is presented here. The laser under study uses three asymmetric Mach-Zehnder interferometers (AMZI) with an electro-optic voltage-controlled phase modulator (PM) in each arm and an additional phase section (Ph) for wavelength tuning [3]. Therefore, it has seven control elements depicted as blue boxes in the schematic in Figure 1. A tuning range of over 50 nm is achieved without changing the amplifier current or the temperature of the chip.

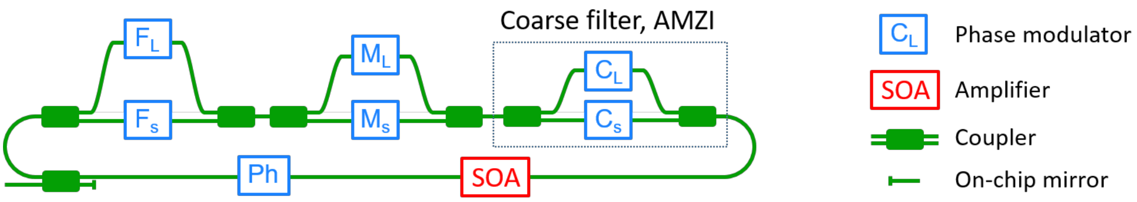

Figure 1 Schematic of the ring laser cavity displaying 7 phase modulators and a semiconductor optical amplifier (SOA). Phase modulators are named according to the filter that they belong to - F(ine), M(edium) and C(oarse), S and L in the index stand for short and long arm, respectively. Ph stands for phase section that is used to control the cavity mode position. AMZI is explained in the introduction text. The on-chip mirror strongly favors one lasing direction over the other, and ensures unidirectional lasing. The schematic is taken from [5] with modified nomenclature.

The maximum thermal power dissipation of 100 µW per voltage-controlled PM gives an advantage over current-based tuning that requires different calibration at different tuning speeds. In comparison, a typical current-operated laser for OCT requires tens of mA [4] signals at approximately 1.5 V, which corresponds to more than two orders of magnitude higher thermal dissipation. High local thermal dissipation acts as a secondary, undesirable tuning mechanism that causes a response at the millisecond timescale, and high currents cause aging through dislocations in the material. Here we present a calibration method for an integrated widely tunable continuous wave InP laser lasing around 1525 nm. The goal is to realize a coarse calibration that will lead to a step-wise scan required for OCT. The calibration presented here is the first step towards reaching a scan that is linear in frequency with 1000 points, 5 GHz apart and 50 kHz repetition rate. A linear scan is desirable because it avoids computationally expensive resampling in k-space when performing Fourier transform to obtain the image.

Methodology

We perform a calibration in two steps. First we simplify the tuning parameter space and establish a coarse tuning map. This laser has 7 tuning elements, these are the PMs shown as blue boxes in Figure 1, and two additional tuning mechanisms that we do not use – the SOA current, kept fixed at 120 mA, and chip temperature, kept at 18°C within 10 mK accuracy. Out of the remaining 7 tuning elements, 3 pairs of PMs that belong to the same AMZI have the same effect on the AMZI tuning, but opposite in sign. In other words, tuning a PM in the long arm of an AMZI will shift the filter transmission to higher wavelengths whereas tuning the PM in the short arm will shift the filter transmission to lower wavelengths, by almost the same amount [5]. This leaves 4 remaining independent PMs. It is most practical to visualize and analyze the effect on laser tuning by scanning the voltages on PMs in groups of two. We first tune the two filters that have the strongest effect on the laser tuning, the PMs in the long arms of the coarse and medium filters (C_L and M_L in Figure 1).

The first tuning map is a 31·31 grid of C_L and M_L voltages with a 0.3 V step. We can map resulting lasing wavelengths onto corresponding voltages. This mapping, linear in first approximation, allows to reduce the number of unknown tuning elements to 2.

The second step is to refine the previously obtained tuning map by tuning the fine filter by controlling F_L. Some of the points obtained in the previous step are then repeated 31 times with 31 different F_L voltages. However, the first calibration step leaves some large gaps in the scan range. Wavelengths within these gaps can be targeted by first setting the control voltages for CL and ML as derived from the linear fits of C_L and M_L obtained in the first calibration step, shown as a dotted line in Figure 2. Then all three filters are tuned by the same amount searching for the missing wavelengths. This results in a refined tuning map with smaller gaps, however the lasing wavelengths obtained in this way are not equidistant in frequency. The spacing varies between 0.03 and 2 nm. This is due to the fact that here we do not attempt to include the phase section Ph in the calibration, which leads to a calibration accurate to at best 5 GHz or 0.04 nm, which corresponds to the cavity free spectral range. In this procedure when tuning the three AMZIs at the same time, the transmission peaks of all the filters are kept aligned. If one control voltage of the filters is changed, the other filters should be tuned in proportion. The proportionality depends on the free spectral range (FSR) of the filters, determined by the degree of asymmetry, given by $\mathrm{FSR} = c/\Delta L_{opt}$, where c is the speed of light and ΔL_{opt} is the optical path length difference of an AMZI [3]. Since the PMs are identical in design, it takes the same amount of voltage $V_{2\pi}$ to change the phase by 2π, which corresponds to tuning the filter over its FSR. In the specific laser design used here that means that if the fine filter is tuned by 7 V the medium filter should be tuned by 0.5 V and the coarse filter should be tuned by approximately 0.05 V.

Finally, to investigate the validity of the tuning map over time we check the set of operating points after 13 days and record the calibration drift, defined as the change in the wavelength from the initial position. The lasing wavelengths are thus recorded at two discrete moments in time and not monitored continuously.

Measurements

As outlined in the Methodology section, we establish the initial tuning map by scanning the M_L and C_L voltages independently from 0 V to 9 V in 30 steps of 0.3 V. During this measurement all the other PM are held at 0 V, the chip temperature is stabilized at 18°C and the SOA is biased with 120 mA. For every of the 961 operation points a spectrum is recorded with a 0.05 nm resolution using the Yokogawa AQ6375 optical spectrum analyzer. Operating points are selected based on the side mode suppression ratio (SMSR) above 30 dB (maximum SMSR is 44 dB). Approximately two thirds of the spectra satisfy this condition. In searching for missing wavelengths to fill in the gaps in the tuning range, the F_L voltage was scanned from 0 to 9 V in steps of 0.3 V. The other filters were scanned simultaneously as described above.

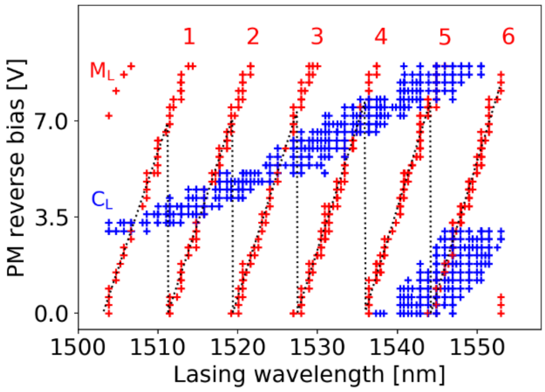

Table 1 Tuning characteristics of the medium-long PM (M_L) seen in figure on the left.

Slope index (see fig.)	Tuning efficiency [nm/V]	Switching voltage $V_{2\pi}$ [V]
1	0.856	6.936
2	0.877	6.951
3	0.910	7.111
4	0.908	7.367
5	0.939	7.690
6	0.951	7.742

Figure 2 Tuning map of the laser, when scanning C_L and M_L and selecting for SMSR higher than 30 dB. C_L voltage is shown in blue and M_L in red. The voltages applied to M_L of the medium AMZI filter with a free spectral range of approximately 7 nm, displayed in red, show the periodicity and the approximate linearity of this tuning mechanism.

The first step in calibration for M_L and C_L voltages is obtained from the data depicted in Figure 2 by performing a series of linear fits. The tuning efficiency and tuning period $V_{2\pi}$ are shown in the table beside Figure 2. Note that a single voltage applied M_L maps to several equidistant lasing frequencies because of the periodicity of the AMZI filter [3].

We inspect the stability of this tuning map over time by repeating the measurement for 500 operating points after 13 days. For every operating point the difference in lasing wavelength before and after is recorded and shown in the histogram in Figure 3a. The histogram shows that the wavelength of 52% of the operating points drift by an integer multiple of the periodicity of one of the filters, 0.5 nm for the fine and 7 nm for the medium AMZI [5]. In principle the drift could be caused by a change in the material, environmental changes, a hysteresis effect in tuning the laser or a sensitivity of this particular laser design to small variations in control signals with respect to the lasing wavelength.

Over the tuning range of 50 nm the gain profile slope changes and different slope could cause an operating point to be more or less likely to drift over time. To test this hypothesis, we plot the change in wavelength of the investigated operating points as a function of wavelength and gain profile slope in Figure 3b. If this hypothesis is true, we would expect to see a higher probability of drift towards the edges of the tuning range where the gain profile slope is sharper, which is not the case.

To test the hysteresis hypothesis we select one operating point and then alternate between this point and a randomly chosen operating point 20 times, while monitoring for a change in wavelength and SMSR. Wavelength changes as large as those in Figure 3a are not observed for this operating point. However further investigation is required before this cause of wavelength change can be ruled out. A similar approach was used to check if variations in temperature and bias current can cause drift of a single operating point. However we observed no large (bigger than 0.1nm) wavelength change for a variation of

± 0.5° or ± 0.5 mA. These variations in current and temperate are larger than expected under typical operating conditions.

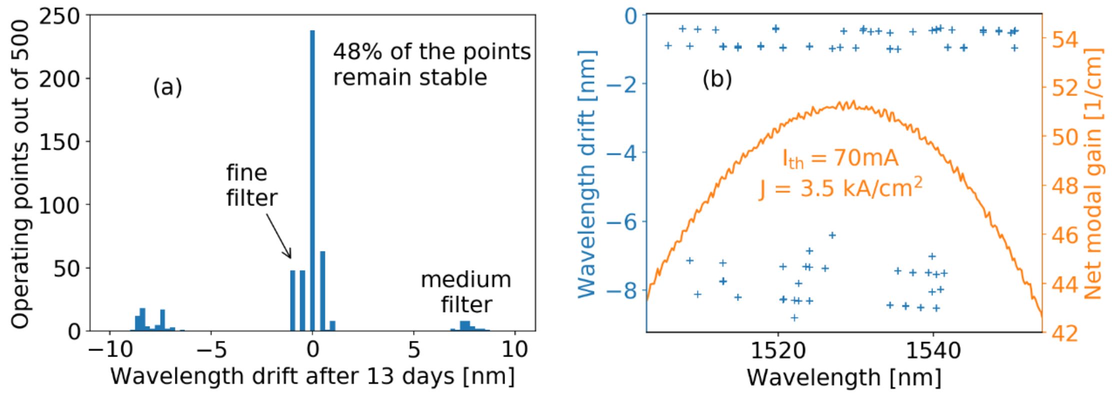

Figure 3 Histogram with 0.25 nm bins showing calibration drift (left) and wavelength drift versus gain profile from [6].

Finally we tune the phase section (Ph) and monitor the output spectrum of the laser with 100 MHz resolution using APEX 2041A optical spectrum analyzer. Ph is expected to only shift the cavity modes and, when tuned over the switching voltage of $V_{2\pi}$, to cause the well-known rollover between two neighboring longitudinal modes. However we observe complex change in the output spectrum with lasing wavelength changes of up to 0.5 nm. The change in spectrum is consistent with a small change in the tuning of the fine filter which implies that there is some electrical coupling between the PMs involved. Previous measurements show that tuning the long arm of the fine tuning AMZI is more efficient than tuning the short arm of the same filter [5]. This observation supports the hypothesis that the applied voltage is not confined only to the PM electrode, since otherwise equal PMs show different effective length.

Conclusions

We show how a two-step calibration can be used to reach a coarse tuning map. To reach the precision tuning required for OCT the problem of electrical cross-talk between phase modulators needs to be addressed through fabrication or design.

Acknowledgements

This project has received funding from the European Union's Horizon 2020 research and innovation program under the Marie Skłodowska-Curie grant agreement No. 721766.

References

[1] M. Smit et al., "An introduction to InP-based generic integration technology," Semiconductor Science and Technology, vol. 29, no. 8, p. 083001, 2014.

[2] S. Schneider et al., "Optical coherence tomography system mass-producible on a silicon photonic chip," Optics Express, vol. 24, no. 2, pp. 1573–1586, 2016.

[3] S. Latkowski et al., "Novel widely tunable monolithically integrated laser source," IEEE Photonics Journal, vol. 7, no. 6, pp. 1–9, 2015.

[4] D. J. Derickson et al., "SGDBR single-chip wavelength tunable lasers for swept source OCT," in Proceedings of SPIE, 2008, vol. 6847.

[5] R. Pajković et al., "Tuning of an integrated tunable laser for swept source optical coherence tomography," 22nd Annual Symposium of the IEEE Photonics Benelux Chapter, pp. 164-167, 2017.

[6] D. Pustakhod, K. Williams, and X. Leijtens, "Fast and robust method for measuring semiconductor optical amplifier gain," IEEE Journal of Selected Topics in Quantum Electronics, vol. 24, no. 1, pp. 1–9, 2017.